

Discovering Sparse Counterfactual Factors via Latent Adjustment for Survey-based Community Intervention

Fatima Ashraf, Muhammad Ayub Sabir, Junbiao Pang*, Yufang Zhou, and Yan Shang

Abstract—Transportation surveys are widely used to understand travel preferences and adoption barriers, yet most survey-based analyses remain descriptive or predictive and rarely provide sparse, policy-feasible intervention strategies. We study sparse counterfactual community intervention from survey responses, where the goal is to shift a target respondent group toward a desired reference group through controllable survey-variable adjustments. We formulate this task as a policy-feasible distributional alignment problem using a fixed-basis nonnegative latent representation that preserves pre/post comparability and provides a stable map from latent factors to original variables. To make latent movement actionable, target-relevant latent factors are identified through Shapley-guided attribution and transferred to controllable variables as intervention priorities. Feasible group-level adjustments are then learned by minimizing an entropy-regularized optimal-transport discrepancy between the post-intervention target distribution and the reference distribution, together with a weighted $\ell_{2,1}$ penalty that promotes shared policy-lever sparsity. Experiments on real-world transportation survey datasets show that the proposed framework produces compact and interpretable policy-feasible interventions with explicit adjustment magnitudes, improves population-level conversion, and preserves intervention sparsity. Code and datasets are publicly available at: <https://github.com/pangjunbiao/latent-group-alignment.git>.

Index Terms—Counterfactual intervention, optimal transport, latent space, Shapley value, sparse optimization

I. INTRODUCTION

Surveys are widely used to study adoption-related intentions, behavioral barriers, and respondent heterogeneity in public programs, services, and technologies [1], [2], [3]. In transportation settings, for example, large-scale questionnaires help agencies understand who adopts transit, why travel decisions are made, and which controllable factors may shape stated intention under practical constraints [4], [5], [6]. However, most survey-based analyses remain descriptive, explanatory, or predictive: they identify factors associated with adoption intention, but rarely provide a principled mechanism for learning sparse and feasible interventions from survey responses [7], [8], [9].

This gap motivates the problem of sparse counterfactual community intervention, where the objective is to shift a target population toward a desired reference population through policy-feasible adjustments on controllable survey variables.

Existing methods address only fragments of this problem. Structural equation modeling and discrete choice models, including SEM and mixed logit, are effective for estimating latent constructs, structural relationships, and heterogeneous behavioral effects [10], [11]. However, they typically stop at

explanation or factor identification, without producing optimized interventions that specify which controllable variables should be adjusted jointly and by what magnitude. Recent counterfactual and distributional methods move closer to intervention design, but they are primarily developed for instance-level recourse or predictive distribution shifts rather than population-level, survey-based interventions under mixed-type feasibility constraints [12]–[14]. The key missing capability is therefore an integrated methodology that converts survey evidence into sparse, feasible, and interpretable group-level interventions.

This task is challenging for three coupled reasons. First, survey responses are heterogeneous and mixed-type, making direct group comparisons in the original feature space unreliable. Second, latent factors can reveal coherent respondent structure, but they are not actionable unless their importance can be stably and consistently mapped back to controllable variables. Third, community intervention must move a target group toward a reference group at the distribution level while respecting immutable attributes, mixed-type validity, and sparsity constraints.

We address these challenges through a conversion-by-alignment framework. It begins by representing encoded survey responses in a fixed-coordinate latent space. We instantiate this representation with fixed-basis NMF because its nonnegative additive factors match the encoded survey domain and its loading matrix provides a stable map from latent factors to original variables. The basis is kept fixed so that pre- and post-intervention respondents are compared under the same latent coordinates.

Within this fixed latent space, outcome-anchored clustering identifies the desired reference group and the target group, and both groups are represented as empirical distributions rather than centroids. To make latent movement actionable, we train a transparent logistic surrogate only as a latent-outcome association probe and use Shapley attribution to obtain target-group latent-factor relevance. These latent priorities are then transferred through the fixed NMF basis to controllable survey variables. Finally, we learn sparse feasible adjustments by minimizing an entropy-regularized OT discrepancy between the post-intervention target distribution and the reference distribution, together with a weighted $\ell_{2,1}$ penalty that promotes shared policy-lever sparsity.

The main contributions of this paper are as follows:

- We formulate survey-based community intervention as a sparse, policy-feasible distributional alignment problem that shifts a target group toward a reference group through

Email: * Corresponding author, junbiao_pang@bjut.edu.cn

controllable survey-variable adjustments in a fixed latent space.

- We develop a target-aware latent-to-feature prioritization mechanism, where a transparent logistic surrogate and Shapley attribution identify important latent factors and transfer them through the fixed basis to controllable feature priorities.
- We propose a sparse feasible distributional intervention objective that combines entropic OT alignment with weighted $\ell_{2,1}$ shared-lever sparsity to produce compact, interpretable, and policy-feasible adjustments.

II. RELATED WORK

A. Survey-Based Perception and Intention Analysis in Public Transportation

Recent studies have examined public-transport perception mainly through analysis of service quality, satisfaction, and behavioral intention. De Oña and de Oña [10] used SEM and SEM-MIMIC on private-vehicle users across five European metropolitan areas and showed that involvement is a key latent factor affecting behavioral intention, while also revealing substantial heterogeneity across user groups. Rong et al. [15] combined passenger satisfaction surveys with actual bus traveling-performance data and, using gradient boosting decision trees, showed that passenger perception does not directly mirror objective service performance but follows a complex nonlinear relationship. Ye and Sato [16] analyzed private-car user’s willingness to switch to public transportation through SEM and found that psychological benefits of public transport promote switching intention, whereas favorable perceptions of private cars suppress it. At a broader level, Sogbe et al. [17] synthesized 104 studies on bus transport usage in developing countries and identified safety, reliability, comfort, and accessibility as core determinants of public-transport usage, while also highlighting issues such as first-mile/last-mile connectivity and behavioral heterogeneity. Overall, this line of work identifies key perceptual factors and explains differences in public-transport adoption. However, it does not provide a sparse, actionable intervention over controllable variables.

B. Latent-Factor and Topic-Based Representation in Transportation Data

Recent studies have used topic-based and latent-factor methods to uncover hidden structure in transportation-related data. Ashraf et al. [18] proposed an importance-aware topic-modeling framework for public-transit risk discovery from noisy social media, showing that low-rank topic structure and topic-localized residual interactions can be jointly recovered for interpretable risk characterization. Li et al. [19] applied BERTopic to large-scale social-media discourse and showed that topic-based semantic modeling can reveal recurring public concerns, psychological barriers, and service expectations related to urban transit adoption. Yang et al. [20] used NMF on large-scale mobility visitation data to represent urban lifestyles as mixtures of latent patterns not fully explained by demographics. Aminpour and Saidi [21] applied Latent Dirichlet Allocation

to transit smart-card and land-use data to infer detailed non-home/work activity patterns, showing that topic models can recover interpretable mobility structure beyond simple trip-purpose categories. Kriswardhana et al. [11] combined latent class analysis and structural equation modeling to identify heterogeneous public-transport user profiles and showed that the effects of service quality, satisfaction, involvement, and prior knowledge vary across traveler groups.

These studies show that topic-based and latent-factor models are effective for discovering structure, heterogeneity, and interpretable representations in mobility and transit data. However, they focus on representation and profiling, and do not connect latent representations to actionable intervention over controllable survey factors.

C. Explainable AI and Counterfactual Explanation Methods

Recent explainable-AI research has increasingly used counterfactual reasoning to generate actionable explanations through structured feature or latent-space adjustments. Na et al. [22] generated practical and plausible counterfactuals by minimally adjusting semantic information in a disentangled latent space, while Crupi et al. [14] proposed latent-space interventions that improve the feasibility and causal consistency of counterfactual recommendations. Kim et al. [23] further showed that incorporating dependencies among related features can improve the plausibility and coherence of counterfactual changes beyond feature-independent perturbations. In the transportation domain, Wang et al. [12] combined deep traffic forecasting with multi-objective counterfactual optimization to explain how contextual variables affect traffic-speed predictions under spatial, temporal, and scenario constraints.

Overall, these studies show that counterfactual reasoning can move beyond feature attribution toward feasible and interpretable explanation mechanisms. However, they are primarily designed for instance-level recourse or model explainability, rather than survey-based group conversion with controllable policy levers and sparse feasible intervention design.

III. METHODOLOGY

A. Policy-Feasible Survey Intervention Problem

We consider a survey dataset comprising n respondents and d encoded features. Each respondent i is represented by a nonnegative vector $x_i \in \mathbb{R}_+^d$, and the full survey matrix is $X = [x_1^\top, \dots, x_n^\top]^\top \in \mathbb{R}_+^{n \times d}$. The nonnegative representation is used not only as preprocessing, but also to provide a common domain for ordinal, one-hot, and numeric survey variables while preserving feature-level interpretability.

This work differs from standard survey modeling and instance-level counterfactual explanation. Rather than only identifying variables associated with an outcome or generating isolated individual recourse [24], we seek sparse and feasible changes to controllable survey variables that move a low-outcome target group toward a desired reference group at the population level. Since survey variables have different measurement semantics, intervention feasibility must be defined before any latent modeling or optimization is introduced.

To structure the heterogeneous survey responses, the encoded features are first partitioned by measurement type:

$$\{1, \dots, d\} = S_{\text{Lik}} \cup S_{\text{Cat}} \cup S_{\text{Num}}, \quad (1)$$

where S_{Lik} , S_{Cat} , and S_{Num} denote Likert, categorical one-hot, and numeric variables, respectively. Binary variables are treated as a special subset $S_{\text{Bin}} \subseteq S_{\text{Num}}$. This measurement-type partitioning allows the framework to handle mixed-type survey data appropriately, enforcing type-specific feasibility constraints during interventions.

To distinguish actionable levers from immutable attributes, we further partition the feature indices as

$$\{1, \dots, d\} = S_{\text{ctrl}} \cup S_{\text{fixed}}, \quad S_{\text{ctrl}} \cap S_{\text{fixed}} = \emptyset, \quad (2)$$

where S_{ctrl} indexes controllable factors and S_{fixed} indexes immutable attributes. This distinction is critical: not all influential variables can be directly intervened upon, and policy feasibility requires that interventions only modify controllable features.

Problem. Let $\Delta_i \in \mathbb{R}^d$ denote the intervention applied to respondent i , and let $\Delta = [\Delta_1^\top, \dots, \Delta_n^\top]^\top \in \mathbb{R}^{n \times d}$ denote the full intervention matrix. The post-intervention feature vector for respondent i is $x_i^{\text{post}} = x_i + \Delta_i$. Given a target group B and a desired reference group A , our goal is to learn a sparse, feasible intervention Δ over S_{ctrl} that shifts the post-intervention target distribution toward the reference distribution, while leaving non-target respondents and the reference group unchanged. The intervention must respect the following feasibility constraints:

- (i) **Immutability:** $\Delta_{ij} = 0$ for all i and $j \in S_{\text{fixed}}$.
- (ii) **Mixed-type validity:** x_i^{post} must remain valid under the encoded survey representation. Specifically, Likert variables must remain within admissible ordinal ranges, numeric variables within feasible intervals, categorical one-hot blocks are not directly modified, and binary controllable variables are relaxed to $[0, 1]$ during optimization and rounded to $\{0, 1\}$ when reporting interventions.

Thus, the intervention problem is not defined by predictive relevance alone, but by the joint requirements of actionability, mixed-type validity, group-level distributional movement, and sparse policy implementation.

B. Fixed-Coordinate Latent Representation

The encoded survey space is heterogeneous and often high-dimensional, making direct group comparison in the original feature space difficult to interpret. We therefore evaluate group structure and intervention effects in a lower-dimensional latent space. However, not every latent representation is suitable for distributional counterfactual intervention. In our setting, the latent space must satisfy three requirements: compatibility with nonnegative encoded survey responses, an interpretable link between latent factors and original variables, and a fixed coordinate system in which pre- and post-intervention respondents remain comparable.

We employ standard NMF as a representational tool to construct this latent space [25]. NMF is used because its nonnegative additive factors are compatible with the encoded

survey representation, and its explicit loading matrix provides a stable map from latent coordinates back to original variables.

Other latent models could be used only if they keep the same fixed coordinates and provide such a stable latent-to-feature map. Unlike signed linear bases or nonlinear embeddings, NMF offers a simple and interpretable way to satisfy these requirements for nonnegative survey responses.

Specifically, the encoded survey matrix X is factorized as

$$X \approx WH, \quad W \in \mathbb{R}_+^{n \times k}, \quad H \in \mathbb{R}_+^{k \times d}, \quad k \ll \min(n, d), \quad (3)$$

where the i -th row w_i^\top of W is the latent representation of respondent i , and the r -th row of H describes the loading pattern of latent factor r over the encoded features.

The key design choice is to keep the basis H fixed after it is learned from the observed survey data. This fixed-coordinate design is necessary because the intervention changes x_i , but the meaning of each latent factor must remain unchanged. If the basis were re-learned after intervention, a change in latent coordinates could reflect either a real respondent movement or a change in the coordinate system itself, making pre/post comparison ambiguous. By fixing H , every observed and post-intervention respondent is represented using the same latent factors, so movement in latent space has a consistent interpretation.

Because NMF is scale-ambiguous, we normalize each row of H to unit ℓ_1 norm and absorb scale into W . Since group identification and optimal-transport alignment depend on relative latent composition, we use row-normalized coefficients $\tilde{w}_i = w_i / \|w_i\|_1$.

For any post-intervention feature vector $x_i^{\text{post}} = x_i + \Delta_i$, its latent representation is obtained by projection onto the fixed basis via nonnegative least squares (NNLS):

$$w_i^{\text{post}} = \arg \min_{w \geq 0} \|x_i^{\text{post}} - wH\|_2^2. \quad (4)$$

Thus, fixing H does not freeze respondent positions in latent space; post-intervention respondents can still move through their updated coefficients w_i^{post} , while the basis remains a common reference frame.

The normalized post-intervention coefficient is $\tilde{w}_i^{\text{post}} = w_i^{\text{post}} / \|w_i^{\text{post}}\|_1$. Thus, interventions are applied in the original feature space, while effects are measured as stable, interpretable movement from \tilde{w}_i to $\tilde{w}_i^{\text{post}}$ in the shared fixed latent space. This fixed-coordinate representation provides the common geometry used for group identification, latent-to-feature prioritization, and distributional alignment.

C. Outcome-Anchored Latent Group Distributions

Community intervention requires shifting a target group toward a reference group; therefore, we first identify coherent respondent groups in the shared latent space. The normalized latent representations \tilde{w}_i from Sec. III-B encode relative latent composition and provide a fixed-coordinate geometry for group comparison.

We apply k -means clustering to $\{\tilde{w}_i\}_{i=1}^n$ with G clusters, yielding assignments $g(i) \in \{1, \dots, G\}$ and cluster index sets

$\mathcal{S}_c = \{i : g(i) = c\}$. These clusters capture latent response patterns, but latent structure alone does not determine which group should serve as the intervention target or the desired reference group. To resolve this, we anchor the clusters to the observed survey outcome. Let y_i denote the primary outcome score, and define the cluster-wise mean

$$\bar{y}(c) = \frac{1}{|\mathcal{S}_c|} \sum_{i \in \mathcal{S}_c} y_i. \quad (5)$$

The cluster with the highest mean outcome is selected as the reference group, $A = \arg \max_c \bar{y}(c)$, while the cluster with the lowest mean outcome is selected as the target group, $B = \arg \min_c \bar{y}(c)$. Their respondent index sets are denoted by \mathcal{S}_A and \mathcal{S}_B , respectively. This outcome anchoring separates latent representation from intervention role assignment: clustering identifies coherent respondent structure, while the outcome determines which latent group represents the desired direction and which group defines the intervention target.

Having identified the target and reference groups, we represent them as empirical distributions rather than single centroids. This distributional representation is essential because the intervention objective aims to shift a population distribution while preserving within-group heterogeneity, which cannot be captured by a single mean vector. Formally, we define

$$\mu_A = \frac{1}{|\mathcal{S}_A|} \sum_{j \in \mathcal{S}_A} \delta_{\tilde{w}_j}, \quad \mu_B = \frac{1}{|\mathcal{S}_B|} \sum_{i \in \mathcal{S}_B} \delta_{\tilde{w}_i}, \quad (6)$$

where δ_w denotes the Dirac mass at location w . These empirical measures define the group distributions used later for optimal-transport alignment. Unlike centroid-based representations, they preserve the variability and heterogeneity of respondents within each group.

D. Target-Aware Latent-to-Feature Prioritization

The target and reference distributions define the desired population shift, but they do not specify which controllable survey variables should be prioritized for intervention. This step is critical because the group structure exists in latent space, while feasible policy actions must operate directly on the original encoded survey variables. We therefore need a bridge from outcome-relevant latent factors to actionable feature-level priorities.

To identify outcome-relevant latent factors, we use a transparent latent-outcome probe. Specifically, we train a surrogate model on normalized latent coefficients \tilde{w}_i to predict a binarized outcome label $y_i^{\text{bin}} \in \{0, 1\}$ derived from y_i (see Supplementary Sec. S1):

$$\hat{y}_i = f(\tilde{w}_i), \quad f : \mathbb{R}_+^k \rightarrow [0, 1]. \quad (7)$$

We use logistic regression for f because the purpose of the surrogate is not to build a high-capacity predictor, but to obtain a stable and transparent association between the fixed latent coordinates and the survey outcome. Since each input dimension of f corresponds to a fixed latent factor, Shapley attribution can be interpreted directly as latent-factor relevance [26]. The surrogate is therefore not treated as a causal model or the final

intervention objective; it serves only as an outcome-association probe for prioritizing latent factors before mapping them back to controllable variables.

For each respondent i and latent factor $r \in \{1, \dots, k\}$, let $\phi_r^{(i)}$ denote the local Shapley value of factor r for the prediction $f(\tilde{w}_i)$. Since interventions target the low-outcome group, we aggregate local attributions over \mathcal{S}_B to obtain target-group-specific latent-factor relevance:

$$\varphi_r = \frac{1}{|\mathcal{S}_B|} \sum_{i \in \mathcal{S}_B} |\phi_r^{(i)}|. \quad (8)$$

The absolute value ensures that φ_r reflects the magnitude of predictive relevance irrespective of direction, focusing on feature importance rather than effect sign. The top- q most relevant latent factors form the set:

$$\mathcal{K}_q = \text{Top-}q(\{1, \dots, k\}; \varphi_r). \quad (9)$$

These selected latent factors are then mapped to actionable feature priorities using the fixed NMF basis H from Sec. III-B, where $H_{r,j}$ denotes the loading of feature j on latent factor r . Each controllable feature $j \in \mathcal{S}_{\text{ctrl}}$ receives a priority score:

$$\omega_j = \sum_{r \in \mathcal{K}_q} \varphi_r H_{r,j}. \quad (10)$$

A large ω_j indicates that controllable feature j has high loading, through the fixed basis H , on latent factors relevant to the target-group outcome. Thus, ω_j is not a causal effect estimate; it is a target-aware priority used to guide sparse intervention optimization. This latent-to-feature transfer is possible because the latent coordinates and feature loadings remain fixed across observed and post-intervention respondents.

E. Sparse Feasible Distributional Intervention

Given the target and reference distributions (μ_B, μ_A) from Sec. III-C and the controllable-feature priorities $\{\omega_j\}_{j \in \mathcal{S}_{\text{ctrl}}}$ from Sec. III-D, the final step is to learn an intervention that is feasible in the original survey-feature space and effective in the fixed latent space. Let $\Delta \in \mathbb{R}^{n \times d}$ denote the intervention matrix, with post-intervention response vector $x_i^{\text{post}} = x_i + \Delta_i$. Interventions are applied only to the target group and must satisfy the actionability and mixed-type validity constraints defined in Sec. III-A. We denote the corresponding feasible set by C :

$$C = \left\{ \Delta \in \mathbb{R}^{n \times d} : \begin{aligned} &\Delta_i = 0, \quad \forall i \notin \mathcal{S}_B, \\ &\Delta_{ij} = 0, \quad \forall j \in \mathcal{S}_{\text{fixed}} \cup \mathcal{S}_{\text{Cat}}, \\ &x_i + \Delta_i \text{ remains feasible, } \forall i \in \mathcal{S}_B \end{aligned} \right\}. \quad (11)$$

For any $\Delta \in C$, each post-intervention target respondent is projected onto the fixed basis H using Eq. (4), yielding normalized latent code $\tilde{w}_i^{\text{post}}$. The resulting post-intervention target distribution is

$$\mu_B^{\text{post}}(\Delta) = \frac{1}{|\mathcal{S}_B|} \sum_{i \in \mathcal{S}_B} \delta_{\tilde{w}_i^{\text{post}}}. \quad (12)$$

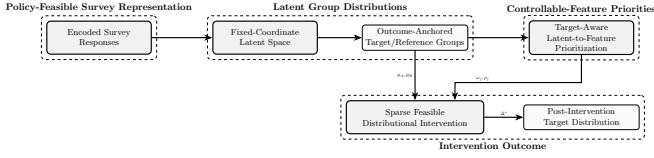


Fig. 1: Overview of the conversion-by-alignment framework for survey-based community intervention.

Thus, the intervention is optimized in the original feature space, but its population-level effect is evaluated as movement of $\mu_B^{\text{post}}(\Delta)$ toward μ_A in the fixed latent space.

Because both groups are represented as empirical distributions in the fixed latent space, the alignment criterion must compare full distributions rather than only individual points or group means. We therefore use entropic optimal transport to measure the minimum latent-space transport cost required to move the post-intervention target distribution toward the reference distribution [27].

Let $\mathcal{S}_A = \{a_q\}_{q=1}^{n_A}$ and $\mathcal{S}_B = \{b_p\}_{p=1}^{n_B}$. The intervention-dependent ground cost is

$$M_{pq}(\Delta) = \|\tilde{w}_{b_p}^{\text{post}} - \tilde{w}_{a_q}\|_2^2. \quad (13)$$

This ground cost is computed in the fixed latent space, so distances measure respondent similarity under a shared coordinate system.

The entropic OT discrepancy is

$$W_\eta(\mu_B^{\text{post}}(\Delta), \mu_A) = \min_{\Gamma \in \mathbb{R}_+^{n_B \times n_A}} \langle \Gamma, M(\Delta) \rangle + \eta \sum_{p,q} \Gamma_{pq} (\log \Gamma_{pq} - 1), \quad (14)$$

subject to

$$\Gamma \mathbf{1} = \frac{1}{n_B} \mathbf{1}, \quad \Gamma^\top \mathbf{1} = \frac{1}{n_A} \mathbf{1},$$

where Γ is the transport plan and $\eta > 0$ controls entropic smoothing. Unlike centroid matching, this objective aligns empirical distributions and therefore accounts for within-group heterogeneity. The entropy term provides a smoother and more stable alignment objective for optimization.

Distributional alignment alone may spread changes across many variables. To obtain policy-realistic interventions, we impose weighted shared-lever sparsity:

$$\Omega(\Delta; \rho) = \sum_{j \in \mathcal{S}_{\text{ctrl}}} \rho_j \|\Delta_{:,j}\|_2, \quad \rho_j = (\omega_j + \epsilon_\omega)^{-1}. \quad (15)$$

Here $\|\Delta_{:,j}\|_2$ measures the population-level adjustment magnitude of controllable feature j . The $\ell_{2,1}$ structure encourages the intervention to activate a compact set of shared policy levers, while the weights ρ_j reduce the penalty on target-relevant features identified in Sec. III-D.

The final intervention is obtained by solving

$$\min_{\Delta \in C} W_\eta(\mu_B^{\text{post}}(\Delta), \mu_A) + \lambda \Omega(\Delta; \rho), \quad (16)$$

where $\lambda > 0$ balances distributional alignment and sparse policy implementation. This objective combines the central requirements of the framework: feasible feature-space adjustment, fixed-coordinate latent evaluation, distribution-level movement toward the reference group, and sparse shared policy levers.

The optimization is nonconvex because Δ affects the latent distribution through the fixed-basis projection in Eq. (4). We solve it using an auxiliary-variable penalized relaxation with post-intervention latent codes U and alternating projected proximal updates. Projection onto C maintains feasibility at each update. Detailed update rules and convergence criteria are provided in the Supplementary Material (Sec. I). An overview of the proposed framework is shown in Fig. 1, and the overall procedure is summarized in Algorithm 1.

Algorithm 1 Conversion-by-Alignment Framework

Require: Encoded feature matrix $X \in \mathbb{R}_+^{n \times d}$; controllable/fixed partitions $\mathcal{S}_{\text{ctrl}}, \mathcal{S}_{\text{fixed}}$; outcome scores $\{y_i\}_{i=1}^n$; NMF rank k ; cluster number G ; OT regularization η ; sparsity weight λ

Ensure: Sparse counterfactual intervention Δ^* and active policy levers

- 1: Factorize $X \approx WH$ using (3); fix H and obtain row-normalized latent representations \tilde{w}_i .
 - 2: Cluster $\{\tilde{w}_i\}_{i=1}^n$ into G groups; define reference group A and target group B using (5).
 - 3: Construct empirical group distributions μ_A and μ_B using (6).
 - 4: Train the latent-outcome surrogate f using (7); compute local Shapley values $\phi_r^{(i)}$, aggregate ϕ_r using (8), select \mathcal{K}_q using (9), and compute feature priorities ω_j using (10).
 - 5: Define feasible set C using (11); initialize $\Delta^{(0)} = 0$ with support restricted to $\mathcal{S}_B \times \mathcal{S}_{\text{ctrl}}$.
 - 6: Initialize auxiliary latent codes $U^{(0)} \in \mathbb{R}_+^{n_B \times k}$ and set $\rho_j = (\omega_j + \epsilon_\omega)^{-1}$ for $j \in \mathcal{S}_{\text{ctrl}}$.
 - 7: **for** $t = 0, 1, \dots$ until convergence **do**
 - 8: Update latent codes $U^{(t+1)}$ via projected gradient step (Supp. Sec. I).
 - 9: Update intervention $\Delta_B^{(t+1)}$ via projected proximal-gradient step with weighted $\ell_{2,1}$ regularization (Supp. Sec. I).
 - 10: Project onto C and evaluate $\mathcal{J}(\Delta^{(t+1)}, U^{(t+1)})$ for convergence.
 - 11: **end for**
 - 12: Set Δ^* to the final feasible intervention and return active levers $\{j : \|\Delta_{:,j}^*\|_2 > 0\}$.
-

IV. RESULTS AND DISCUSSION

A. Dataset and Evaluation Metrics

1) Dataset

The primary dataset is a real-world questionnaire survey conducted in Beijing to study public-transport adoption, stated behavioral intention, and responses to carbon-incentive mechanisms. It contains 1021 respondents and 40 raw survey fields. After excluding two non-analytic fields (respondent identifier and contact information), the dataset retains 38 substantive variables spanning attitudes, incentive preferences, reward-response behavior, and respondent background attributes (Table I). To examine generality beyond this setting, we also consider MNIST as a controlled toy domain and the VTA 2013 on-board transit

survey [28] as a second real-world survey dataset.

TABLE I: Summary of the Beijing and VTA survey datasets.

Beijing Survey	
Survey respondents	1021
Raw survey fields	40
Excluded non-analytic fields	2
Substantive variables	38
Survey domain	Public transport carbon-incentive behavior
Variable types	Attitudinal / Incentive / Behavioral / Demographic
VTA Survey	
Survey records	9654
Raw survey fields	85
Survey domain	On-board transit behavior and service evaluation
Variable types	Trip / Access-Transfer / Fare / Rating / Demographic

At the raw-variable level, the Beijing survey consists of four parts: (i) attitudinal and intention-related items, (ii) policy and incentive items, (iii) reward-response items under different incentive levels, and (iv) demographic and contextual attributes such as occupation, education, income, vehicle ownership, residential district, destination district, and transit-card usage. This structure is well suited to latent-factor modeling because the observed survey responses are heterogeneous but partially driven by shared underlying preferences. In particular, attitudinal items, incentive preferences, and reward-response variables can be interpreted as observable manifestations of a smaller set of adoption-related latent factors, while demographic and contextual attributes provide background information that remains fixed under intervention.

The VTA dataset is a real-world on-board transit survey conducted in 2013 to study rider travel behavior, service evaluation, and transit-use characteristics. The dataset contains 9,654 survey records and 85 raw fields, covering trip origins and destinations, access and egress modes, transfer behavior, fare payment, service-quality ratings, transit-use frequency, demographic attributes, language background, vehicle availability, and stated alternatives if VTA transit were unavailable. This structure provides both service-related variables that can be treated as potentially actionable factors and respondent-specific background attributes that remain fixed, making the dataset suitable for evaluating group-level behavioral shift in a second real-world survey domain.

2) Evaluation Metrics

The proposed framework aims to learn a minimal, policy-feasible intervention that moves the target group toward the reference (green-accepting) group. Accordingly, we evaluate both intervention effectiveness and intervention cost.

We use respondent-level conversion as the primary outcome. Let \mathcal{S}_B denote the target group and let $n_B = |\mathcal{S}_B|$. Using the surrogate score $f(\cdot)$ on normalized latent representations, a target-group respondent is counted as converted if the predicted score crosses a decision threshold τ_y after intervention. The number of converted respondents is

$$N_{\text{conv}} = \sum_{i \in \mathcal{S}_B} \mathbf{1}\{f(\tilde{w}_i) < \tau_y \text{ and } f(\tilde{w}_i^{\text{post}}) \geq \tau_y\}, \quad (17)$$

and the corresponding conversion rate is $R_{\text{conv}} = N_{\text{conv}}/n_B$. In

our experiments, we use $\tau_y = 0.5$, which is the standard decision threshold for the logistic-regression surrogate.

Intervention effort is measured by the group-sparse magnitude of the learned adjustment:

$$\|\Delta^*\|_{2,1} = \sum_{j \in \mathcal{S}_{\text{ctrl}}} \|\Delta_{:,j}^*\|_2, \quad (18)$$

which quantifies the total change applied across controllable policy levers. Policy sparsity is further characterized by the number of activated levers:

$$N_{\text{lever}}(\tau_\Delta) = \sum_{j \in \mathcal{S}_{\text{ctrl}}} \mathbf{1}\{\|\Delta_{:,j}^*\|_2 > \tau_\Delta\}, \quad (19)$$

where τ_Δ is a small numerical tolerance used to distinguish active levers from negligible changes. In our experiments, we set $\tau_\Delta = 10^{-6}$.

To measure intervention efficiency, we define

$$\text{Eff}_{\text{conv}} = \frac{N_{\text{conv}}}{\|\Delta^*\|_{2,1}}, \quad (20)$$

which reports the number of converted respondents per unit intervention effort.

To evaluate latent-space alignment, we report the reduction in entropic OT discrepancy between the target and reference distributions. Let

$$W_\eta^{\text{before}} = W_\eta(\mu_B, \mu_A), \quad W_\eta^{\text{after}} = W_\eta(\mu_B^{\text{post}}(\Delta^*), \mu_A). \quad (21)$$

We measure alignment improvement by the absolute reduction $\Delta W_\eta = W_\eta^{\text{before}} - W_\eta^{\text{after}}$, and by the relative reduction $\rho_\eta = \frac{\Delta W_\eta}{W_\eta^{\text{before}}}$. These provide complementary views of how effectively the learned intervention aligns the target distribution with the reference distribution.

B. Model Performance on the Survey Dataset

The proposed framework demonstrates strong effectiveness in moving the target group toward the green-accepting reference group. In the main reference run, the intervention yields 61 conversions out of 355 target respondents, together with a consistent increase in predicted adoption probability and a clear reduction in latent-space discrepancy between the two groups. This indicates that the learned intervention does not merely improve individual surrogate scores, but also moves the overall target distribution closer to the reference group in the learned latent representation. At the same time, the intervention remains sparse and interpretable. Only 8 policy levers are activated, indicating that the observed shift is achieved through focused adjustments rather than broad changes across variables.

Across multiple random seeds (42-45), the same overall pattern is observed: the intervention consistently improves conversion and alignment while maintaining a sparse structure, as shown in Table II.

TABLE II: Performance of the proposed method on the survey dataset.

Setting	$N_{\text{conv}} \uparrow$	$R_{\text{conv}} \uparrow$	Mean $\Delta\rho \uparrow$	$N_{\text{lever}} \downarrow$	Effort ($\ \Delta\ _{2,1}$) \downarrow	$\Delta W_\eta \uparrow$	$\rho_\eta \uparrow$
Seed 42	61	0.1718	0.0365	8	15.6777	0.1090	0.2425
Mean \pm Std	40.25 ± 15.42	0.1233 ± 0.0344	0.0239 ± 0.0088	8.00 ± 0.00	14.8455 ± 0.6057	-	0.2122 ± 0.0367

C. Comparison with Baselines and Ablations

a) Baselines.

- **Top-Shapley Single-Lever:** This intervenes on only one controllable variable, namely the lever with the highest Shapley importance. It represents the simplest importance-based intervention rule and tests whether acting on only the single most influential lever is sufficient to induce meaningful group-level movement.
- **Top-Shapley Top- k Uniform:** This selects the top- k controllable levers according to Shapley importance and applies the same uniform intervention to all of them. It tests whether importance ranking alone is enough, without solving the structured optimization problem used in the full method.
- **Max-Coverage Top- k Uniform:** This baseline selects the k levers with the broadest feasible coverage across the target group and applies a uniform intervention over them. It tests whether choosing widely applicable levers is more effective than choosing importance-ranked levers.
- **Outcome-Only Sparse:** This baseline performs a sparse intervention guided only by the direct outcome objective, without the optimal-transport alignment term. It tests whether improving the surrogate outcome alone is sufficient, or whether explicit distributional movement toward the reference group is necessary.

Table III shows that simple ranking-based or coverage-based intervention rules produce only limited improvement. Although some baselines achieve lower effort or activate fewer levers, they remain clearly below the full method in conversion, mean probability lift, and latent alignment improvement. This indicates that identifying important levers alone is not sufficient; the intervention must also be designed to move the target group toward the reference group in the learned latent space.

TABLE III: Baselines comparison on survey dataset

Method	$N_{\text{conv}} \uparrow$	$R_{\text{conv}} \uparrow$	Mean $\Delta p \uparrow$	Effort ($\ \Delta^*\ _{2,1}$) \downarrow	$N_{\text{lever}}(\tau) \downarrow$	$\Delta W_\eta \uparrow$	$\rho_\eta \uparrow$
Full method	61	0.1718	0.0365	15.6777	8	0.1090	0.2425
Top-Shapley Single-Lever	14	0.0394	0.0096	3.7683	1	0.0296	0.0657
Top-Shapley Top- k Uniform	36	0.1014	0.0214	9.4207	5	0.0641	0.1444
Max-Coverage Top- k Uniform	33	0.0930	0.0194	9.4207	5	0.0579	0.1304
Outcome-Only Sparse	9	0.0254	0.0045	9.4207	5	0.0143	0.0286

b) Ablations.

- **w/o Shapley weighting:** Removes the Shapley-guided lever weighting and tests whether transferring latent importance back to actionable policy levers is necessary.
- **w/o sparsity:** Removes the sparsity-inducing regularization and tests whether the method can remain effective while preserving a compact and interpretable intervention set.
- **w/o OT alignment:** Removes the optimal-transport alignment objective and tests whether distribution-level matching is necessary beyond simpler alignment criteria.

Table IV shows that the full method depends on the interaction of all major components. Removing Shapley weighting leads to the most severe degradation, indicating that principled prioritization of controllable levers is central to the method.

Removing sparsity preserves much of the raw conversion performance, but does so at the cost of activating nearly all controllable levers, which substantially weakens interpretability and policy realism. Removing OT alignment also slightly reduces conversion and alignment performance, confirming that explicit distributional matching contributes beyond optimizing the surrogate outcome alone.

TABLE IV: Ablation study of the proposed method.

Method	$N_{\text{conv}} \uparrow$	$R_{\text{conv}} \uparrow$	Mean $\Delta p \uparrow$	Effort ($\ \Delta^*\ _{2,1}$) \downarrow	$N_{\text{lever}}(\tau) \downarrow$	$\Delta W_\eta \uparrow$	$\rho_\eta \uparrow$
Full method	61	0.1718	0.0365	15.6777	8	0.1090	0.2425
w/o Shapley weighting	8	0.0225	0.0041	2.1102	7	0.0127	0.0281
w/o sparsity	59	0.1662	0.0358	19.3677	32	0.1069	0.2375
w/o OT alignment	59	0.1662	0.0356	19.3677	32	0.1059	0.2357

D. Sensitivity Analysis

To assess the robustness of the proposed framework, we conduct a targeted sensitivity analysis over three key hyperparameters: the latent dimension (k), the number of clusters (G), and the sparsity weight ($\lambda_{2,1}$). These parameters control, respectively, (i) the capacity of the latent representation, (ii) the granularity of group structure, and (iii) the strength of sparsity regularization.

The latent dimension k controls how much structure can be captured in the learned latent representation. When k is too small, the representation is too limited to separate meaningful patterns, resulting in negligible intervention effects. As shown in Table V, increasing k improves performance, with $k = 10$ giving the strongest overall results among the tested settings.

TABLE V: Sensitivity analysis over latent dimension (k), number of clusters (G), and sparsity weight ($\lambda_{2,1}$).

Parameter	Value	N_{conv}	R_{conv}	Mean Δp	$N_{\text{lever}}(\tau)$	Effort ($\ \Delta\ _{2,1}$)	ρ_η	Best Total Obj.	Status
Latent Dim (k)	4	0	0.0000	0.0010	9	1.296	0.0009	–	Weak
	6	0	0.0000	0.0150	5	9.631	0.0347	–	Weak
	8	18	0.0650	0.0168	6	9.887	0.1075	–	Moderate
	10	61	0.1718	0.0365	8	15.678	0.2425	–	Best
Clusters (G)	3	61	0.1718	0.0365	8	15.678	0.2425	–	Best
	5	5	0.0370	0.0095	3	3.224	0.0113	–	Weak
	7	11	0.0753	0.0393	8	10.044	0.0093	–	Weak
	9	0	0.0000	0.0406	32	5.994	-0.0127	–	Unstable
$\lambda_{2,1}$ (Sparsity)	0.05	61	0.1718	0.0365	8	15.6777	0.2425	0.2188	Strong
	0.10	6	0.0169	0.0019	6	0.9652	0.0130	0.2997	Over-reg.
	0.15	0	0.0000	0.0005	6	0.9391	0.0029	0.3015	Failed
	0.20	0	0.0000	0.0005	6	0.9391	0.0029	0.3033	Failed

G determines how finely respondents are partitioned in latent space. A moderate value produces stable and interpretable group structure, while larger values fragment the population, reducing intervention stability and effectiveness. In particular, Table V shows that $G = 3$ gives the strongest results, while larger values reduce stability and, in the case of $G = 9$, lead to ineffective or unstable behavior.

The sparsity weight $\lambda_{2,1}$ controls the trade-off between intervention strength and intervention simplicity. Lower values allow effective yet compact interventions, whereas higher values overly constrain the solution, suppressing conversion and probability gains. This shows that sparsity is important for interpretability, but excessive regularization weakens the intervention itself.

E. SOTA Analysis

A direct state-of-the-art (SOTA) comparison for our problem setting is not available, since existing counterfactual explanation methods are primarily designed for instance-level recourse rather than population-level intervention. To establish a principled empirical reference, we select two representative comparison methods aligned with key aspects of our formulation: (i) CEILS [14], which incorporates causal structure for instance-level recourse, and (ii) DCE [13], which performs distribution-level optimization using optimal transport.

CEILS learns a structural causal model from a user-specified graph and generates counterfactuals either in the observed feature space (“Original”) or in a latent residual space (“CEILS”), which are mapped back through structural equations. As an instance-level method, it provides individual recourse actions. We adapt CEILS to our survey setting using a compatible feature subset, a simplified causal graph, and feasibility constraints over mutable and immutable variables. As shown later in Table VI, both instance-level methods achieve identical conversion performance, indicating that incorporating causal structure alone does not substantially improve behavioral conversion in this setting.

TABLE VI: Comparison with representative counterfactual reference methods on the survey dataset.

Method	Setting	Eval. Size	N_{conv}	R_{conv}	Notes
Original	Instance	165	27	0.1636	Standard CF (no causality)
CEILS	Instance	165	27	0.1636	Causal CF (SCM-based)
DCE (OT-based)	Distribution	33	3	0.0909	OT-based CF (test-set subset)
Ours	Population	355	61	0.1718	Sparse OT-based group intervention

DCE serves as a distribution-level reference because it also adopts an optimal-transport-based objective. However, DCE was originally developed for distributional counterfactual explanation rather than survey-based policy intervention. In our adaptation, we define target and reference groups based on the observed outcome, restrict mutable variables to controllable survey attributes, and enforce feasibility constraints over mixed-type variables. Due to the mismatch between DCE’s native formulation and the structured constraints of survey-based intervention, DCE is evaluated on a reduced compatible test-set subset. In addition, the optimization does not always find fully feasible solutions under these constraints and may rely on the best approximate feasible output. Therefore, its results should be interpreted as a practical distributional counterfactual reference rather than a directly matched population-intervention baseline.

As shown in Table VI, DCE achieves limited conversion ($N_{\text{conv}} = 3$, $R_{\text{conv}} = 0.0909$). This reflects the gap between distributional counterfactual alignment and the requirement of structured, policy-feasible intervention under mixed-type survey constraints.

The compared methods operate at different intervention levels, as reflected in Tables VI and VII. Original and CEILS modify each sample individually, while DCE operates on batches of samples. In contrast, the proposed method learns one coordinated intervention for the full target group.

The lower effort of the reference methods therefore reflects small, localized counterfactual changes rather than a shared

TABLE VII: Intervention characteristics of the compared reference methods.

Method	Statistic Type	Active Levers	Effort
Original	Avg. per instance	3.22	2.0367
CEILS	Avg. per instance	2.85	2.0379
DCE (OT-based)	Avg. per batch sample	0.18	0.1818
Ours	Group-level intervention	8	15.6777

population-level policy action. Although the proposed method has higher total effort, it explicitly models target-aware factor importance and shared intervention magnitude through Shapley-guided prioritization and sparse optimal-transport alignment, making the learned intervention more suitable for practical group-level policy design.

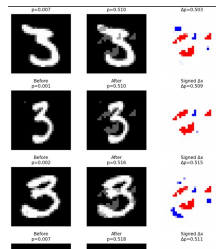
F. Generalization Across Domains

On MNIST, we treat the task as a source-to-target shift problem between two digit classes (3→8). In this setting, each image is treated as an individual sample, where the source digit class represents the initial group and the target digit class serves as the reference group. The intervention is implemented as a constrained perturbation over editable pixel features, and conversion is measured by whether the modified sample transitions toward the target class under the classifier. The results in Table VIII show that the method achieves strong conversion and probability lift in this simplified domain, although the intervention involves a relatively large number of editable features and higher overall effort due to the high-dimensional pixel space.

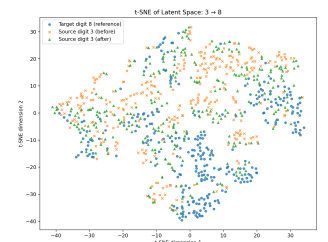
TABLE VIII: Generalization results on MNIST and the VTA survey.

Dataset	Task	N_{conv}	R_{conv}	Mean Δp	Effort ($\ \Delta\ _{2,1}$)	Active Levers	ΔW	ρ
MNIST (3→8)	Image-level shift	200	0.40	0.401	619.30	80	4.43	0.416
VTA Survey	Behavioral shift	733	0.227	0.265	155.02	4	9.03	0.057

More importantly, Fig. 2(b) shows that post-intervention samples move in latent space toward the target-digit region, providing geometric evidence of the intended source-to-target transition. Fig. 2(a) illustrates representative successful conversions, where minimal structured perturbations shift digit 3 toward digit 8. Additional qualitative examples, full-grid visualizations, and signed perturbation maps are provided in the Supplementary Material (Fig. 1 & 2)



(a) Successful conversions (3→8).



(b) t-SNE visualization of latent-space movement.

Fig. 2: MNIST 3→8 conversion: representative samples and latent-space movement.

For the VTA survey, we formulate the task as a group-to-group conversion problem based on rider satisfaction. Each survey respondent is treated as an individual sample, where users with lower satisfaction (Q7F) form the target group and higher-satisfaction users define the reference group. The intervention operates over a restricted set of service-related controllable variables (e.g., Q7A–Q7E), while demographic and contextual attributes remain fixed. The results in Table VIII show that the method achieves consistent conversion and probability improvement, while activating only a small number of policy levers, indicating that sparse and interpretable interventions can be obtained in a real-world survey setting.

G. Characteristics and Interpretation of the Proposed Method

In addition to aggregate conversion performance, we analyze how the proposed method operates at the group, optimization, and policy levels. Specifically, we examine (i) whether the learned intervention induces coherent movement of the target group toward the reference group in latent space, (ii) whether the optimization procedure produces stable and consistently improving updates, and (iii) whether the resulting intervention can be interpreted as a small set of actionable policy levers. These analyses provide complementary evidence on the effectiveness, stability, and interpretability of the proposed framework.

1) Pre–Post Group Movement Analysis

The proposed method is intended to induce *group-level* movement (target group toward the reference group), not merely to improve individual prediction scores. To test this directly, we perform a pre–post group movement analysis that compares the reference group, the target group before intervention, and the same target group after intervention. Table IX reports three complementary quantities for this purpose: the mean surrogate probability, the centroid distance to the reference group in latent space, and the OT discrepancy to the reference distribution.

TABLE IX: Pre–post group movement analysis on the Beijing survey.

Group	Num. Users	Mean Probability	Dist. to Ref. Centroid	OT Discrepancy to Ref.
Reference	499	0.5703	0.0000	0.0000
Target (Pre)	355	0.4339	0.3735	0.7307
Target (Post)	355	0.4704	0.2829	0.6774

This analysis is important because each quantity captures a different aspect of the intended group shift. The mean probability reflects improvement in the modeled outcome, the centroid distance captures geometric movement of the target group toward the reference group in latent space, and the OT discrepancy measures distribution-level alignment while preserving within-group structure.

Table IX shows that, after intervention, the target group exhibits a higher mean probability, a smaller centroid distance to the reference group, and a lower OT discrepancy. Thus, the learned intervention does not simply increase predicted adoption in isolation; it also shifts the target group closer to the reference group in the latent representation and improves alignment at the distributional level.

TABLE X: Top activated policy levers on the survey dataset

Feature Index	Policy Lever	Δ (Magnitude)	Importance (ω)
7	Exchange for discounted health insurance enrollment	0.311	0.074
5	Exchange for fitness course coupons or trial cards	0.261	0.076
6	Exchange for health check-up packages	0.218	0.075
8	Exchange for personal annual carbon reduction certificate	0.009	0.069
9	Exchange for tree planting / ecological protection projects	0.009	0.068
10	Exchange for donations to public welfare projects	0.008	0.061
13	Group-based low-carbon travel to earn more carbon credits	0.008	0.054
4	Exchange for transportation benefits (bus/metro/shared bike)	0.008	0.042

2) Optimization Behavior

To assess the intervention optimizer, we examine the optimization trajectory over accepted iterations. The left panel of Fig. 3 shows the total objective, which decreases monotonically and stabilizes after approximately 20 iterations, indicating stable convergence without oscillation. The right panel shows the mean surrogate gain, which increases steadily in the early and middle stages and then plateaus, indicating that the learned intervention becomes progressively more effective before reaching saturation.

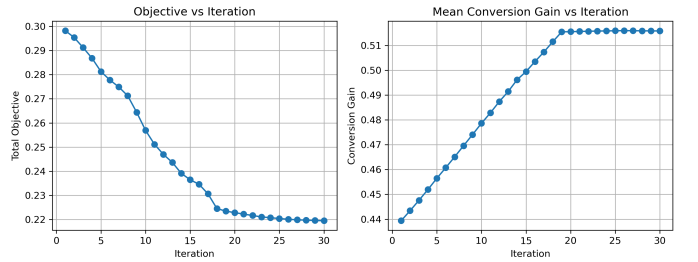


Fig. 3: Optimization trajectory showing monotonic objective decrease and saturation of mean conversion gain across iterations.

Taken together, these trends indicate that the optimization process is stable and well directed: accepted updates consistently improve the objective, while intervention effectiveness increases until no substantial additional gain is obtained. The late-stage plateau in mean surrogate gain suggests that later iterations mainly refine the objective rather than produce large further changes in target-group conversion, supporting convergence to a practically stable solution.

3) Policy-Level Interpretation of the Learned Intervention

A key goal of the proposed framework is not only to improve conversion, but also to identify which controllable policy levers contribute to moving the target group toward the reference group. To make this explicit, Table X reports the active levers selected by the full model, together with their intervention magnitudes and importance weights.

The table shows that the learned intervention is concentrated on a small and interpretable subset of variables rather than being diffused across many features. It also links the final intervention to the latent-to-feature prioritization step, since the most strongly adjusted levers are also assigned relatively high importance weights. This indicates that the optimization is not selecting variables arbitrarily, but is acting consistently on the controllable levers identified as most influential for the modeled outcome. As a result, the learned intervention remains interpretable as a focused set of actionable policy adjustments rather than an opaque high-dimensional modification.

REFERENCES

- [1] M. Srivastava, "A case study and survey-based assessment of the management of innovation and technology," *Journal of technology management & innovation*, vol. 6, no. 1, pp. 147–160, 2011.
- [2] M. N. Borhan, D. Syamsunur, N. Mohd Akhir, M. R. Mat Yazid, A. Ismail, and R. A. Rahmat, "Predicting the use of public transportation: a case study from putrajaya, malaysia," *The Scientific World Journal*, vol. 2014, no. 1, p. 784145, 2014.
- [3] J.-H. Kim, J. Kim, and B.-Y. Youn, "Using a technology acceptance model to explore the intention to use digital health technologies among people with disabilities: cross-sectional survey study," *Journal of Medical Internet Research*, vol. 27, p. e79595, 2025.
- [4] A. J. Yeganeh, R. P. Hall, A. R. Pearce, and S. Hankey, "A social equity analysis of the us public transportation system based on job accessibility," *Journal of Transport and Land Use*, vol. 11, no. 1, pp. 1039–1056, 2018.
- [5] Q.-L. Jing, H.-Z. Liu, W.-Q. Yu, and X. He, "The impact of public transportation on carbon emissions—from the perspective of energy consumption," *Sustainability*, vol. 14, no. 10, p. 6248, 2022.
- [6] H. Susanto, I. N. Hj Ahamad, and A. K. Shafa Susanto, "Investigating consumers' behavioral intentions in the adoption of 5g mobile networks: a holistic approach to technology acceptance and business process integration," *Frontiers in Communications and Networks*, vol. 6, p. 1594378, 2025.
- [7] B. Liu, Z. Ma, H. Kong, and X. Ma, "How incentives affect commuter willingness for public transport: Analysis of travel mode shift across various cities," *Travel Behaviour and Society*, vol. 39, p. 100966, 2025.
- [8] A. Antipova, S. Sultana, Y. Hu, and J. P. Rhudy Jr, "Accessibility and transportation equity," p. 3611, 2020.
- [9] L. Zhang, L. Tao, F. Yang, Y. Bao, and C. Li, "Promoting green transportation through changing behaviors with low-carbon-travel function of digital maps," *Humanities and Social Sciences Communications*, vol. 11, no. 1, pp. 1–10, 2024.
- [10] J. de Oña and R. de Oña, "Is it possible to attract private vehicle users towards public transport? understanding the key role of service quality, satisfaction and involvement on behavioral intentions," *Transportation*, vol. 50, no. 3, pp. 1073–1101, 2023.
- [11] W. Kriswardhana, K. Ismael, S. Duleba, and D. Esztergár-Kiss, "Uncovering distinct public transport user profiles and the factors influencing the users' intentions," *Journal of Urban Mobility*, vol. 7, p. 100127, 2025.
- [12] R. Wang, Y. Xin, Y. Zhang, F. Perez-Cruz, and M. Raubal, "Counterfactual explanations for deep learning-based traffic forecasting," *Communications in Transportation Research*, vol. 5, p. 100176, 2025.
- [13] L. You, L. Cao, M. Nilsson, B. Zhao, and L. Lei, "Distributional counterfactual explanations with optimal transport," *arXiv preprint arXiv:2401.13112*, 2024.
- [14] R. Crupi, A. Castelnovo, D. Regoli, and B. San Miguel Gonzalez, "Counterfactual explanations as interventions in latent space," *Data Mining and Knowledge Discovery*, vol. 38, no. 5, pp. 2733–2769, 2024.
- [15] R. Rong, L. Liu, N. Jia, and S. Ma, "Impact analysis of actual traveling performance on bus passenger's perception and satisfaction," *Transportation Research Part A: Policy and Practice*, vol. 160, pp. 80–100, 2022.
- [16] X. Ye and M. Sato, "Private car users' willingness to switch to public transportation and its influencing factors in the yangtze river delta," *Asian Transport Studies*, vol. 11, p. 100171, 2025.
- [17] E. Sogbe, S. Susilawati, and T. C. Pin, "Scaling up public transport usage: a systematic literature review of service quality, satisfaction and attitude towards bus transport systems in developing countries," *Public Transport*, vol. 17, no. 1, pp. 1–44, 2025.
- [18] F. Ashraf, M. A. Sabir, J. Deng, J. Pang, and H. Yu, "Importance-aware topic modeling for discovering public transit risk from noisy social media," *arXiv preprint arXiv:2512.06293*, 2025.
- [19] X. Li, G. He, P. Guo, Z. Guo, S. Lin, and S. Du, "Topic modeling help enhancing sustainable mobility," *Journal of Cleaner Production*, vol. 534, p. 147068, 2025.
- [20] Y. Yang, A. Pentland, and E. Moro, "Identifying latent activity behaviors and lifestyles using mobility data to describe urban dynamics," *EPJ Data Science*, vol. 12, no. 1, p. 15, 2023.
- [21] N. Aminpour and S. Saidi, "Unveiling mobility patterns beyond home/work activities: A topic modeling approach using transit smart card and land-use data," *Travel Behaviour and Society*, vol. 38, p. 100905, 2025.
- [22] S.-H. Na, W.-J. Nam, and S.-W. Lee, "Toward practical and plausible counterfactual explanation through latent adjustment in disentangled space," *Expert Systems with Applications*, vol. 233, p. 120982, 2023.
- [23] H.-D. Kim, Y.-J. Ju, J.-H. Hong, and S.-W. Lee, "Cirf: Importance of related features for plausible counterfactual explanations," *Information Sciences*, vol. 678, p. 120974, 2024.
- [24] S. Verma, V. Boonsanong, M. Hoang, K. Hines, J. Dickerson, and C. Shah, "Counterfactual explanations and algorithmic recourses for machine learning: A review," *ACM Computing Surveys*, vol. 56, no. 12, pp. 1–42, 2024.
- [25] F. Saberi-Movahed, K. Berahmand, R. Sheikhpour, Y. Li, S. Pan, and M. Jalili, "Nonnegative matrix factorization in dimensionality reduction: A survey," *ACM Computing Surveys*, vol. 58, no. 5, pp. 1–41, 2025.
- [26] E. Borgonovo, E. Plischke, and G. Rabitti, "The many shapley values for explainable artificial intelligence: A sensitivity analysis perspective," *European Journal of Operational Research*, vol. 318, no. 3, pp. 911–926, 2024.
- [27] G. Peyré and M. Cuturi, *Computational optimal transport: With applications to data science*. Now Foundations and Trends, 2019.
- [28] "Santa clara valley on-board transit survey (2013)," <https://www.nlr.gov/transportation/secure-transportation-data/tsdc-santa-clara-valley-onboard-transit-survey>, 2013.